RSC Advances

ROYAL SOCIETY OF CHEMISTRY

www.rsc.org/advances

Cite this: DOI: 10.1039/c0xx00000x

www.rsc.org/xxxxxx

ARTICLE TYPE

Preparation of high performance lithium-ion battery with separator-cathode assembly

Wei Xiao*, Lina Zhao, Yaqun Gong, Shaoliang Wang, Jianguo Liu and Chuanwei Yan

Received (in XXX, XXX) Xth XXXXXXXXX 20XX, Accepted Xth XXXXXXXXX 20XX

DOI: 10.1039/b000000x

In this study, a novel separator-cathode assembly (SCA) comprising a positive electrode and a ceramic separator layer applied to this electrode is facilely prepared and investigated in lithium-ion batteries. The preparation of SCA is performed by directly applying a suspension of polyvinylidene fluoride (PVDF)/Al_2O_3 (acetone as solvent) on the as-prepared cathode by hot spray coating method, which can effectively prevent the adverse effect of coating suspension on the microstructure of the electrode. Systematical investigations including morphology and structure characterization, water wettability testing and thermal resistance property are carried out. The results indicate that the SCA possesses notable features, such as uniform and porous surface morphology, highly developed microporous structure, excellent wettability and thermal stability. Based on the above advantages, the cells assembled with SCA exhibit better electrochemical performances, such as the discharge C-rate capability and cycling performance, as compared to the commercialized PP separator. It is demonstrated that the SCA can availably improve the discharge performance and protect the battery from internal short, which is highly desirable for the development of high power/high energy lithium-ion batteries.

Introduction

Lithium-ion batteries (LIBs) have been the most employed power source in portable electronics[1, 2] Recently, they have been considered as the most powerful candidates for the applications of hybrid and all-electric vehicles. Worldwide research is in progress to develop high energy/high power LIBs for such applications.[3-6] However, the safety problems of LIBs have recently received considerable attention, owing to the increased potential for fire and/or explosion under unwanted conditions, such as hard internal shorts.

Among the various components in LIBs, the separator can separate the positive and negative electrodes and provide the ionic conduction through the liquid electrolyte. Nowadays, the commonly used commercial separators are polyolefin separators. Although these separators have good performance with a reasonable cost, they also have some drawbacks in the application of future energy storage devices.[6, 7] Especially, their low thermal stability and poor wetting property provoke serious concerns over their fundamental functions to ensure electrical isolation and also ionic transport between electrodes.[5]

To enhance the thermal resistance of the separators, alternative separators with improved thermal stability have been developed using thermally stable materials such as brominated poly(phenylene oxide),[8] poly(ethylene terephthalate) (PET),[9] polyimide,[10] and cellulose.[11] More recently, incorporation of inorganic particles into polyolefin-based separators or thermal-resistant polymeric non-wovens has been widely investigated.[12-18] Jung et al [12] coated a thin Al_2O_3 layer (< 10 nm) onto and into the porous PP separator by atomic layer deposition technology. The thin Al_2O_3 coating improved the safety of the battery due to suppressed thermal shrinkage and increased electrolyte uptake. Lee et al [13] prepared SiO_2-embedded composite separator on PET non-woven by dip-coating method. Compared with the polyolefin separator, the composite separator shows superior thermal stability. These polymeric and composite separators exhibit enhanced thermal stability, but their costs are relatively high compared with that of the polyolefin separators.

In order to overcome the above disadvantages of separators and simplify the production of LIBs, ceramic separators have been formed on electrodes directly to prepare the separator-electrode assembly.[19-21] Hoerpel et al [19] provided an all-inorganic separator-electrode assembly in which ceramic particles were used as fillers and inorganic sols were used as binders. Huang[20] coated a bilayer separator (a ceramic layer and a PVDF layer) directly on the anode through a solution casting process. The battery with this separator showed high thermal stability and stable cycling performance. However, the above methods suffer from some drawbacks, such as brittleness, low air permeability and complex process. And the solvents, such as N, N-dimethylformamide (DMF) and N-methyl-2-pyrrolidone (NMP), in which separator coating materials were dispersed, may destroy the structures of the as-prepared electrodes during the separator casting and drying processes.

Based on the high mechanical strength, chemical resistance of PVDF and the thermal resistance, electrolyte wettability of Al_2O_3 particles[7], in this study PVDF/Al_2O_3 composite separator was coated directly on the cathode to prepare separator-cathode

assembly (SCA) for LIBs. To reduce the negative impact of coating suspension on the microstructure of the cathode, volatile acetone was used as solvent to disperse the coating materials. A simple spray coating method was adapted to enhance the uniformity and coverage of the separator on the cathode as well as the adhesion of the separator to the cathode. Compared with the conventional separators, the SCA can endow the battery with low internal resistance and good protection against internal short circuit as well as low cost.

Experimental

Preparation of separator-cathode assembly

The cathode was prepared by mixing $LiFePO_4$ (Tianjin STL Co. Ltd.), acetylene black (Timcal, Switzerland), and polyvinylidene fluoride (PVDF, Kynar 2801) in NMP with a weight ratio of 80:10:10 and pasted on an aluminum current collector of 25 μm thick, and then dried in a vacuum oven at 120 °C for 12 h. The lithium foil (Aldrich) was used as the counter electrode.

The ceramic coating suspension was prepared by mixing PVDF and Al_2O_3 particles (average particle size = 200 nm) in acetone, wherein the PVDF/Al_2O_3 composition ratio was 2: 8. After first dissolving PVDF in acetone at 50 °C , a predetermined amount of Al_2O_3 powder was added and the mixture was then further subjected to vigorous mechanical stirring to form a uniform dispersion. Then the PVDF/Al_2O_3 suspension was applied on the as-prepared cathode by spray coating method using an airbrush operating at 0.3 MPa of compressed air in 30 s. During the coating process, the cathode was maintained at 120 °C using a hot plate in air atmosphere for evaporation of the solvent and densification of the coating layer. The operation parameters of the spray coating process were adjusted so that the formed ceramic separator was about 30 μm. The schematic models of the cathode and the SCA are shown in Fig. 1.

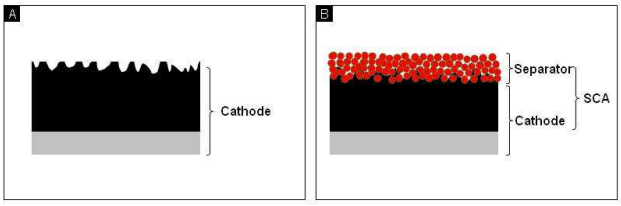

Fig. 1 Schematic diagrams of the cathode and the SCA

To determine the characteristics of the ceramic separator, a free-standing ceramic separator was formed directly on a flat substrate as described in the previous case for the preparation of ceramic separator on the cathode.

Materials Characterization

The morphologies and chemical compositions of the cathode and the SCA were characterized by scanning electron microscopy (FEI INSPECT F) equipped with an energy dispersive X-ray analysis (EDX) microanalyzer. The average pore size of the separator was evaluated using a mercury porosimeter (Auto Pore IV9500, Micromeritics). The porosity of the separator was determined using n-butanol uptake method.[17]

The water contact angles of the cathode and the SCA were measured by the sessile drop method (JC2000C1, Chengde Jinhe Technic Apparatus Co. Ltd., China). The thermal stabilities of the ceramic separator and PP separator were determined by combustion test.

Electrochemical Measurements

For the measurement of the electrochemical performances, a liquid electrolyte of 1M $LiPF_6$ in ethylene carbonate (EC)/diethyl carbonate (DEC) (1/1, v/v, Tinci Materials Technology Co., Ltd., China) was employed. The ionic conductivity of the liquid electrolyte-soaked separator between two stainless-steel plate electrodes was evaluated by an AC impedance analysis (Gamry Reference 600) over a frequency range of 10^{-2}–10^5 Hz at room temperature.

CR2032-type coin cells were assembled in a high-purity argon-filled glove box with the SCA as the cathode/separator, lithium foil as the anode, and 1 M $LiPF_6$ in EC/DEC (1:1) as the electrolyte. For comparison, cells with conventional structure were fabricated by stacking PP separator (Celgard 2400) between $LiFePO_4$ cathode and lithium foil anode followed by injection of the electrolyte. To further investigate the thermal resistance of the SCA, cells with different structures were charged to 4.2 V and then placed in an oven. The cell skin temperature was maintained at 150 ◦C and cell open circuit voltage was recorded. The initial discharge capacity, cycling performance, and discharge C-rate capability of the cells with different structures were investigated using a cycle tester (BTS-5V3mA) under a constant current-constant voltage charge and constant current discharge mode, with a cutoff potential of 4.2 V and 2.5 V at room temperature.

Results and discussion

The structures of LIBs with conventional separator and SCA are compared in Fig. 2. In commercial LIBs, separators and electrodes are generally fabricated separately and only combined by the battery manufacturer at elevate temperature and pressure.[7] In the present LIBs, the SCA and the anode are laminated to produce novel structured battery as shown in Fig. 2 B. Different from the conventional separators, the separator in SCA is applied directly on the cathode by spray coating method which can enhance the adhesion between the electrode and the separator, resulting in low resistance and high mechanical stability. In addition, the porous ceramic separator can provide very good protection against the short circuit of the two electrodes which can never give rise to a meltdown, since the inorganic particles will ensure that the separator does not melt. This technology can also reduce the complexity and cost for manufacturing LIBs. It can be speculated that the battery with SCA can combine the advantages of the liquid electrolyte (high conductivity) and the gel electrolyte (good adhesion to the electrodes) as well as the ceramic separator (excellent thermal resistance).

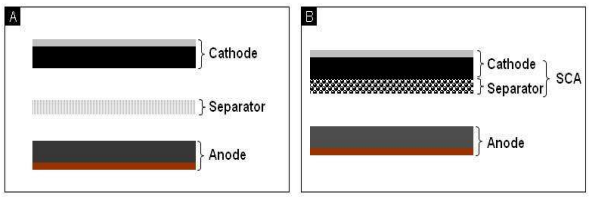

Fig. 2 Comparison of the lithium-ion batteries with conventional separator (A) and separator-cathode assembly (B)

SEM and EDX characterization of the as-prepared cathode and the ceramic coated cathode were conducted to investigate their differences in morphology and structure. Due to the better comprehensive performances, in this work $LiFePO_4$ was used as active material for the cathode. Fig. 3 A shows that the as-prepared cathode has relatively dense and uniform surface morphology. The EDX result confirms that this cathode is mainly comprised of $LiFePO_4$ which is widely used as cathode material in LIBs. By contrast, significantly different morphologies were observed in the SCA as shown in Fig. 3 (C~F).

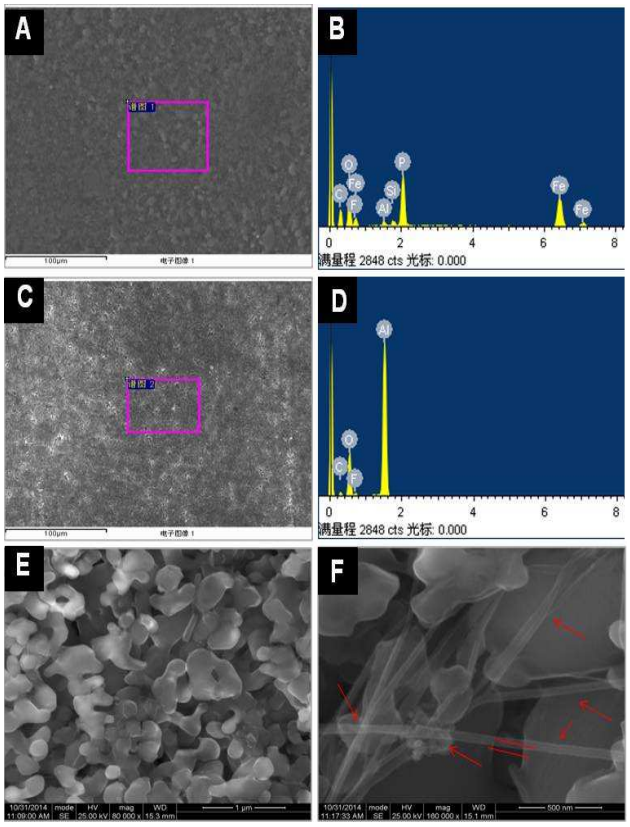

Fig. 3 Surface SEM images and EDX measurements of the as-prepared $LiFePO_4$ cathode (A, B) and the separator-cathode assembly (C-F)

Fig. 3 C and E show that after the spray coating process the ceramic particles are closely packed on the surface of the as-prepared cathode, which allows for the evolution of a ceramic separator with porous structure as that of the reported ceramic composite separator.[13,15] Fig. 3 D confirms the coating layer is mainly consisted of Al_2O_3 particles, moreover, the absence of EDX peaks from Fe and P indicates that the coating layer is continuous enough to completely cover the $LiFePO_4$ layer. Most of the reported ceramic composite separators are fabricated by dip-coating method, in which film-shaped PVDF binder should wrap the inorganic particles and block the pores, resulting in the separator with poor wettability and low ion conductivity.[9] It is found that in this study as binder PVDF is in the form of fiber (50~100 nm) as marked with red lines in Fig. 3 F, which can effectively fasten the Al_2O_3 particles without blocking the micropores in the ceramic separator. This preferable fiber-shaped PVDF binder may result from the spray coating process and the fast evaporation of acetone.

Fig. 4 shows the cross section SEM image and EDX measurements of the separator-cathode assembly. The SCA has three layers as marked in Fig. 4 A. The bottom layer is aluminium current collector with a thickness of about 12 μm. The middle layer is the cathode layer which is comprised of $LiFePO_4$, PVDF and acetylene black. The top layer is the ceramic composite separator which is directly applied on the cathode by spray coating method. It can be seen the ceramic separator is about 30 μm in thickness with good affiliation to the cathode. The corresponding EDX measurements of the three areas also confirm the above statements.

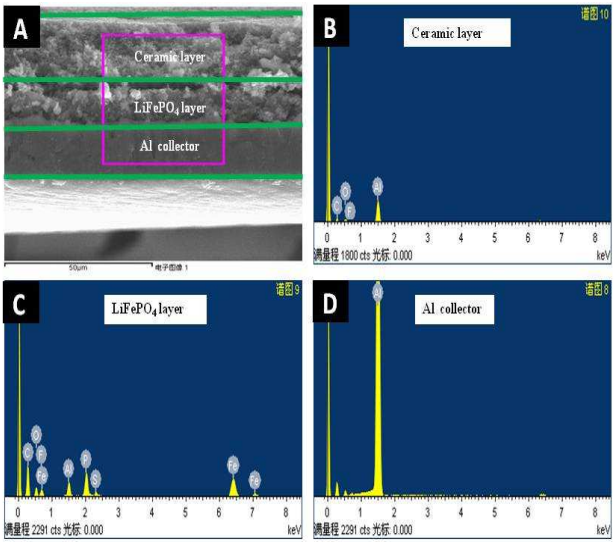

Fig. 4 Cross section SEM image (A) and EDX measurements (B-D) of the separator-cathode assembly

So the Al_2O_3 particles layer applied directly on the cathode will ensure the electrodes separated even at higher temperature and enhance the electrolyte wettability of the SCA due to the porous structure compared with polyolefin separators.

Fig. 5 shows the pore size distribution of the ceramic separator. It is obvious that the separator has mean pore size of about 240 nm with narrow pore size distribution. This microstructure is preferred for the application in lithium-ion batteries.[7]

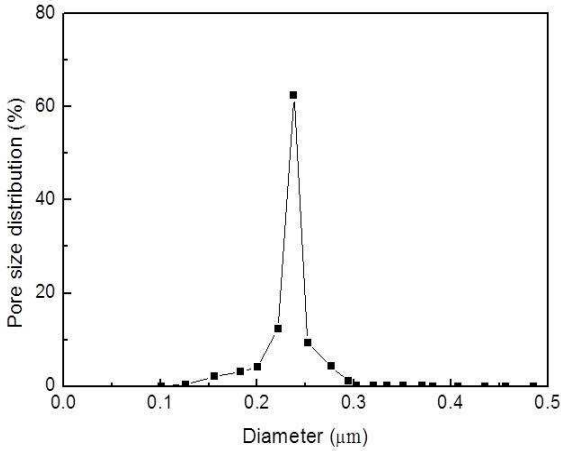

Fig. 5 Pore size distribution of the ceramic separator

Contact angle tests with water droplets were conducted to investigate the effect of ceramic coating on the wettability of the

cathode. As shown in Fig. 6 A, different from the as-prepared $LiFePO_4$ cathode, the color of the separator-cathode assembly is white. Moreover, the ceramic coating layer decreased the contact angle of the as-prepared cathode from 139 ° ± 1.2 ° to 54 ° ± 1.5 °, which is ascribed to the relatively polar (i.e., electrolyte-philic) constituents and the porous structure of the SCA.[2,8] The improvement in contact angle implies that the SCA has better wettability compared to the conventional electrodes and separators, which is beneficial for the applications in LIBs.[11,12]

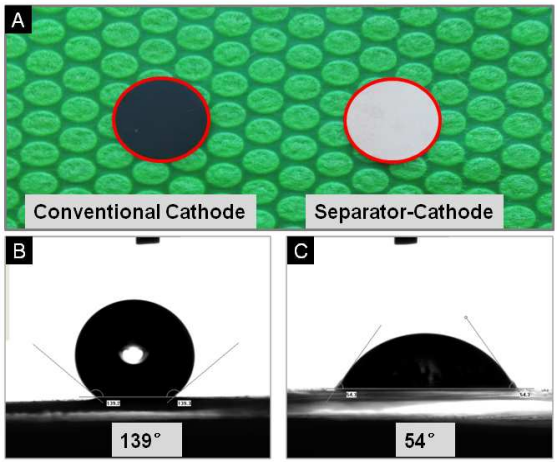

Fig. 6 Photographs of $LiFePO_4$ cathode and separator-cathode assembly (A) and the corresponding water contact angle images (B, C)

The safety of LIBs is closely related to the thermal stability of the separators. At high temperature, the polyolefin separators exhibit large thermal shrinkage, resulting in a short circuit between electrodes.[7] In most of the reported references, the dimensional shrinkages of the separators maintained at high temperature were used to examine their thermal stabilities.[13] In this study, the flammability of the separators was used to determine the thermal resistance of the ceramic separator and the PP separator by combustion test as shown in Fig. 7. Before the combustion test the appearance of the two separators were almost the same. Due to the high flammability of PP material, during the test PP separator burned wildly with blue flame and at last it completely disappeared.

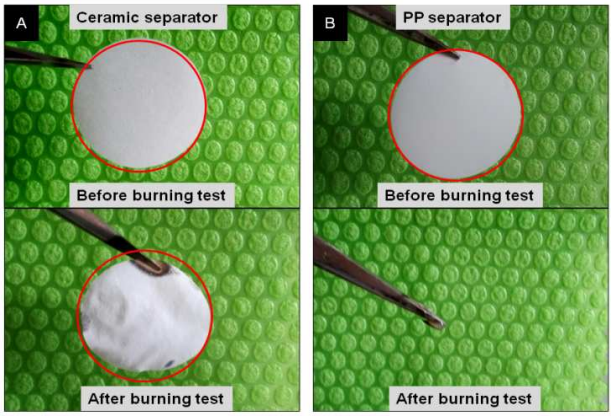

Fig. 7 Combustion test of ceramic separator (A) and PP separator (B)

In contrast, the ceramic separator was shortly burned with yellow flame, indicating incomplete combustion. After the test most of the polymer binder was burned completely and the flameproof ceramic particles were left with separator dimensional shrinkage of only about 10% and mass lose of about 5%. This improvement could be ascribed to the introduction of Al_2O_3 particles into the separator and the unique separator structure induced by the spray coating method.[22] Due to the high thermal stability, the ceramic coating integrated with the cathode can endow the SCA with high thermal resistance, thereby hindering the internal short circuit of LIBs at high temperature. Table 1 lists the basic properties of PP separator and ceramic separator.

Fig. 8 shows the AC impedance spectra of the liquid electrolyte-soaked ceramic separator and PP separator. The AC spectra were typically non-vertical spikes for stainless steel (SS) blocking electrodes, that is, the SS/separator/SS cell. The straight lines inclined towards the Z' axis represents the electrode/ electrolyte double layer capacitance behavior. Thus, the bulk resistance of the separators can be acquired from the high-frequency intercept of the Nyquist plot on the Z' axis (shown in inset curve of Fig. 8).[23] It is found that the bulk resistance of ceramic separator is about 2.87 Ω, which is slightly lower than that of PP separator (4.31 Ω). By considering the thickness of the separator and the area of the locking electrodes, the ionic conductivity (=1.49 $mScm^{-1}$) of ceramic separator is higher than that (=0.65 $mScm^{-1}$) of PP separator.

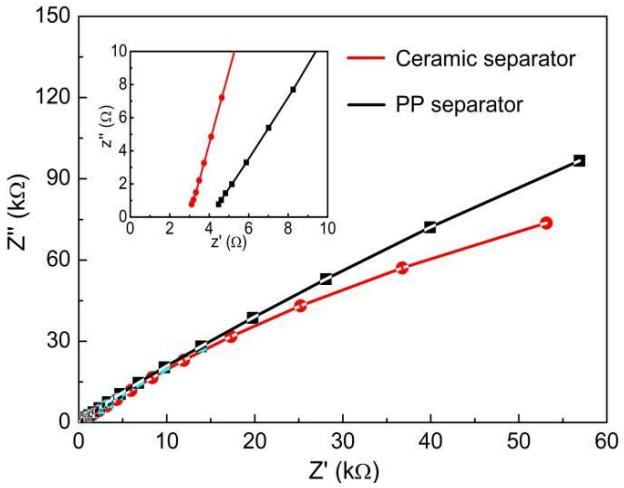

Fig. 8 Nyquist plot of ceramic separator and PP separator at open-circuit potential with an AC voltage of a perturbation signal 5 mV

The higher ionic conductivity of ceramic separator demonstrates that the porous structure in the coating layer is highly developed, and therefore contributes to facile lithium-ion diffusion after being filled with liquid electrolyte. In addition, as reported[24,25] when the Al_2O_3 particles are introduced into separators, the charge and electric field associated with the particles interact with the liquid electrolyte, leading to the formation of a double layer or space charge. And the space charge layer can further promote the conduction of lithium ions.

Open circuit voltage (OCV) drop can reflect the self-discharge behavior of LIBs and predict the risk of internal short circuit. In this test the cells were kept in the heating vessel to induce internal short circuit and self-discharge, and the variations for OCV of the cells were monitored to compare the thermal stabilities of different separators.

Fig. 9 shows that there are remarkable differences in OCV profiles between the cells assembled with PP separator and SCA. The OCV value of the PP cell marginally declines with storage time prolonging and then drops rapidly. After 15 min, the OCV value drops to 2.0 V indicating a "soft short", which is mostly induced by the formation of small localized contact between electrodes, resulting from the slightly shrinkage of PP separator. After 45 min, the OCV value drops to 0 V, which may be explained by the directly contacting of cathode and anode. It is reported that the PP separator showed dimensional shrinkage of about 50% when maintained at about 150 ◦C for 1 h, so in this test the crucial shrinkage of PP separator causes complete internal shout circuit of the cell.

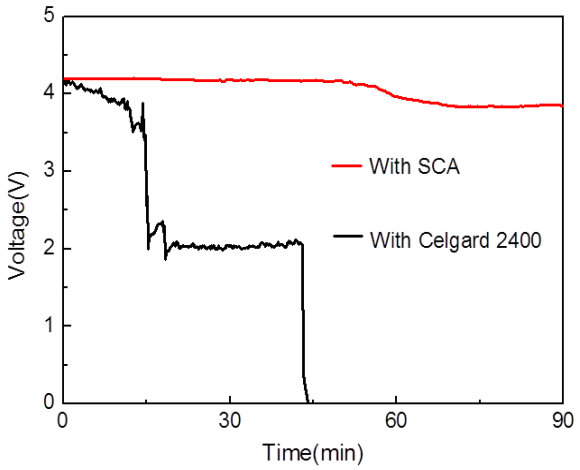

Fig. 9 Open circuit voltage profiles for the cells with SCA and PP separator during the hot oven test at 150 °C for 1.5 h

However, the SCA cell showed a very gentle voltage drop, and no sudden voltage change was observed during the test. After 90 min, the OCV value is still as high as 4.0 V. After the OCV test, it was found that the separator-cathode assembly showed almost no dimensional change, while the area shrinkage of PP separator was up to 30%. So it can be speculated that the sudden voltage drop of the cell with PP separator was caused by the internal short circuit due to the thermal shrinkage of the separator.

The OCV study suggests that the SCA is thermally stable in the liquid electrolyte at high temperature. This may be attributed to the thermal-resistant materials and the unique separator structure, in which the bottom of the ceramic layer is firmly anchored in the cathode surface (as shown in Fig. 1 B) and meanwhile the fiber-shaped binders fasten the particles tightly (as shown in Fig. 3 F).

Charge–discharge curves of the cells in the first cycle at 0.2 C/0.2 C are presented in Fig. 10 A. Two pseudoplateaus at around 3.4 and 3.6 V that indicate the typical electrochemical behaviors of the $LiFePO_4$ spinel were observed in both charge and discharge curves. The PP cell has an initial discharge capacity of 142.1 mAh g^{-1} with a coulombic efficiency of 78.4%. However, the SCA cell exhibits an discharge capacity of 146.3 mAh g^{-1} with a coulombic efficiency of 81.5%, both of which are higher than those of PP separator. Fig. 10 B shows the cycling performance of the cells with different separators at 0.2 C/0.2 C. It is obvious that all of the cells showed similar coulombic efficiencies of about 99% during the cycle tests. However, the SCA cell always has the higher discharge capacity than the PP cell. After 60 cycles, the capacity retention ratio of the SCA cell is about 86% which is higher than that of the PP cell.

Two reasons are attributed to the performance improvement. One is the special battery structure, since the SCA can ensure the firmly contact and interface uniformity between the separator and the electrode and decline the interface resistance. Another reason may be the higher electrolyte wettability and retention ability of the SCA, which can prevent additional decomposition of the liquid electrolyte at both electrode interfaces during cycling processes.[26]

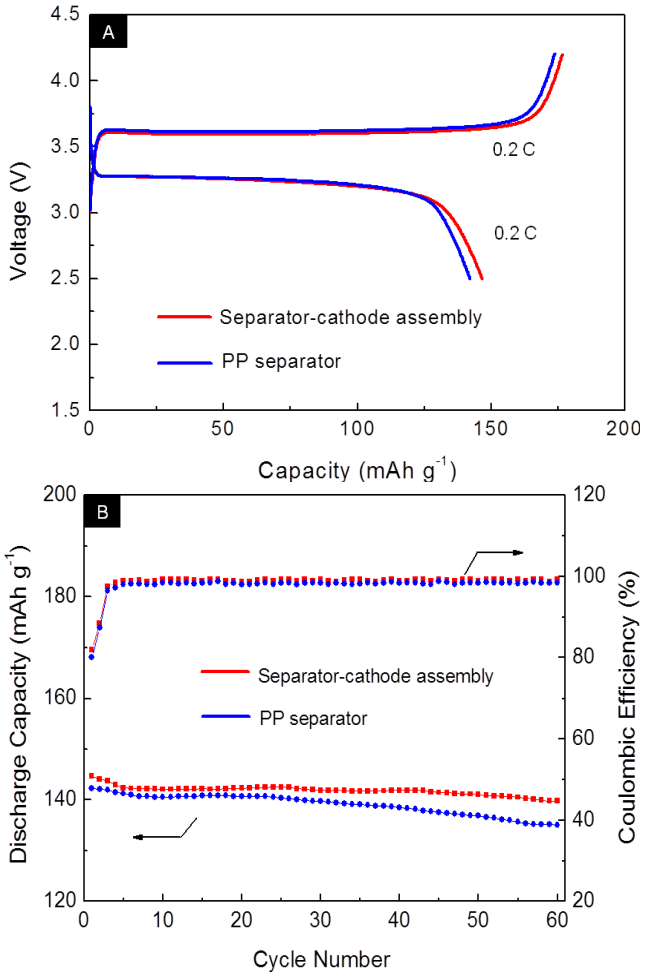

Fig. 10 Initial voltage profiles (A) and cycling performance (B) of the cells with PP separator and separator-cathode assembly at 0.2 C rate

The C-rate capabilities of the cells with different structures have been investigated, in which the cells are cycled at different charge/discharge current densities of 0.5 C/0.5 C, 1.0 C/1.0 C, 2.0 C/2.0 C, 4.0 C/4.0 and 8.0 C/8.0 C. As shown in Fig. 11, as the discharge current density increases, the voltage and discharge capacity of the cells tend to gradually decrease. The discharge C-rate capacities of the SCA cell appear to be higher than those of the PP cell. Moreover, this difference in discharge capacities between the separators becomes larger at higher discharge current densities where the influence of ionic transport on ohmic polarization is significant. [27]

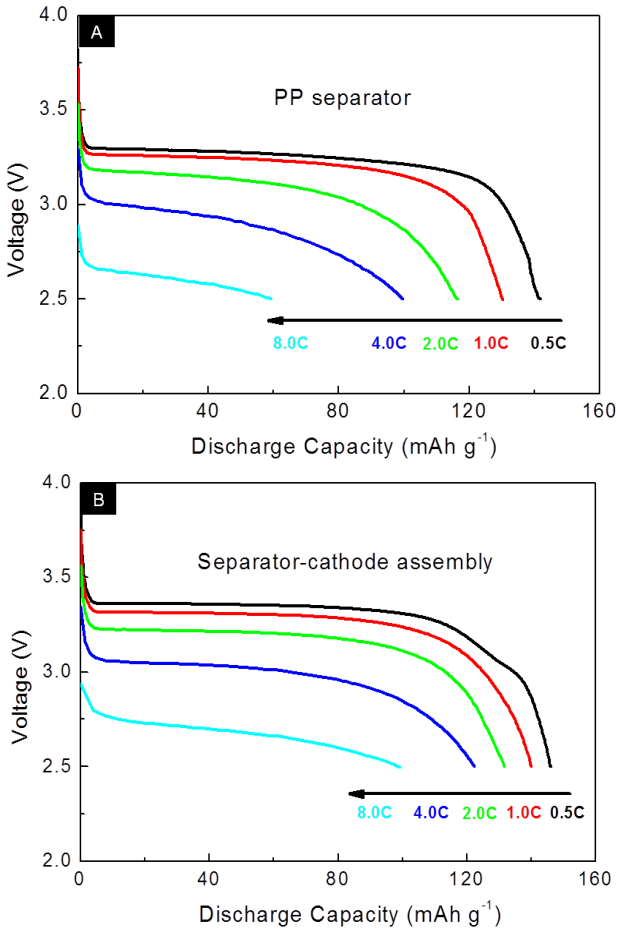

Fig. 11 Dependence of discharge capacity on discharge C-rate of the cells with PP separator (A) and separator-cathode assembly (B)

Comparison of the data in Fig. 11 A and B demonstrates that the SCA cell exhibits much better rate capability as compared to the PP cell at various rates. For example, the SCA cell keeps a specific capacity of 100.1 mA h g^{-1} (about 69% of the discharge capacity at 0.5 C) at 8.0 C, whereas the specific capacity of the PP cell was only 62.4 mA h g^{-1} (about 44% of the discharge capacity at 0.5 C). In addition, compared with the reported ceramic separators,[13-15] this novel SCA endowed the cell with better rate capability, which may be ascribed not only to the lower interfacial resistance (enhanced adhesion of the separator to the cathode) but also to the higher ionic conductivity of the ceramic separator (highly developed porous structure) as shown in Table 1.

Table 1 Basic properties of PP separator and ceramic separator

Sample	Thickness (μm)	Average pore size (nm)	Porosity (%)	Electrolyte uptake (%)
PP separator	25	90	42	124
Ceramic separator	30	240	67	230

Conclusions

With spray coating method and fast evaporation process, a ceramic suspension of PVDF and Al_2O_3 was directly applied on the cathode, resulting in a separator-cathode assembly. Due to the fiber-shaped PVDF binders, the uniformity and coverage of the separator on the cathode as well as the adhesion of the separator to the cathode were enhanced. The lithium-ion battery assembled with the separator-cathode assembly exhibits preferable comprehensive performances, such as the cyclability, C-rate capability and the thermal resistance, compared with the commercial PP separator. In summary, this separator-cathode assembly can function not only as an electrode but also as a high performance separator, resulting in a good candidate for high energy/high power lithium-ion batteries.

Acknowledgments

This work was supported by the National Science Foundation of China (grant no. 21306213).

Notes and references

Laboratory for Corrosion and Protection, Institute of Metal Research, Chinese Academy of Sciences, China.
Tel.: +86 24 2399 8320; fax: +86 24 2388 0201.
E-mail: wxiao@imr.ac.cn

1 V. Etacheri, R. Marom, R. Elazari, G. Salitra and D. Aurbach, Energy Environ. Sci., 2011, **4**, 3243-3262.
2 J. Hassoun, S. Panero, P. Reale and B. Scrosati, Adv. Mater., 2009, **21**, 4807-4810.
3 Y. Ko, H. Yoo and J. Kim, RSC ADV., 2014, **4**, 19229-19233.
4 M. Armand and J. M. Tarascon, Nature, 2008, **451**, 652-657.
5 J. B. Goodenough and K.S. Park, J. Am. Chem. Soc., 2013, **135**, 1167-1176.
6 N. S. Choi, Z. H. Chen, S. A. Freunberger, X. L. Ji, Y. K. Sun, K. Amine, G. Yushin, L. F. Nazar, J. Cho and P. G. Bruce, Angew. Chem. Int. Ed., 2012, **51**, 9994-10024.
7 P. Arora and Z. M. Zhang, Chem. Rev., 2004, **104**, 4419-4462.
8 J. J. Woo, S. H. Nam, S. J. Seo, S. H. Yun, W.B. Kim, T. W. Xu and S. H. Moon, Electrochemistry Communications, 2013, **35**, 68-71.
9 E. S. Choi and S. Y. Lee, J. Mater. Chem., 2011, **21**, 14747-14754.
10 W. Jiang, Z. H. Liu, Q. S. Kong, J. H. Yao, C. J. Zhang, P. X. Han and G. L. Cui, Solid State Ionics, 2013, **232**, 44-48.
11 M. Baginska, B. J. Blaiszik, R. J. Merriman, N. R. Sottos, J. S. Moore, and S. R. White, Adv. Energy Mater., 2012, **2**, 583-590.
12 Y. S. Jung, A. S. Cavanagh, L. Gedvilas, N. E. Widjonarko, I. D. Scott, S. H. Lee, G. H. Kim, S. M. George and A. C. Dillon, Adv. Energy Mater., 2012, **2**, 1022-1027.
13 H. S. Jeong, E. S. Choi and S. Y. Lee, J. Membr. Sci., 2012, **415**, 513-519.
14 K. Prasanna, T. Subburaj, W. J. Lee and C. W. Lee, Electrochimica Acta, 2014, **137,** 273-279.
15 C. C. Yang, Y. C. Chen, Z. Y. Lian, T. H. Liou, J. Y. Shih, J. Solid State Electrochem., 2012, **16**, 1815-1821.
16 D. Fu, B. Luan, S. Argue, M. N. Bureau and I. J. Davidson, J. Power Sources, 2012, **206**, 325-333.
17 M. Yanilmaz, M. Dirican and X. W. Zhang, Electrochimica Acta, 2014, **133**, 501-508.
18 M. Raja and A. M. Stephan, RSC ADV., 2014, **4**, 58546-58552.
19 G. Hoerpel, V. Hennige, C. Hying and S. Augustin, US 8163441B2.
20 X. S. Huang, J. Power Sources, 2011, **196**, 8125-8128.
21 S. S. Zhang, K. Xu, D. L. Foster, M. H. Ervin and T. R. Jow, J. Power Sources, 2004, **125**, 114-118.
22 J. H. Park, J. H Cho, W. Park, D. Ryoo, S. J. Yoon, J. H. Kim, Y. U. Jeong and S. Y. Lee, J. Power Sources, 2010, **195**, 8306-8310.
23 M. Xia, Q. Z. Liu, Z. Zhou, Y. F. Tao, M. F. Li, K. Liu, Z. H. Wu and D. Wang, J. Power Sources, 2014, **266**, 29-35.
24 B. Kumar, J. Power Sources, 2004, **135**, 215-231.
25 P. Zhang, L. C. Yang, L. L. Li, M. L. Ding, Y. P. Wu and R. Holze, J. Membr. Sci., 2011, **379**, 80-85.
26 H. S. Jeong, J. H. Kim and S.Y. Lee, J. Mater. Chem., 2010, **20**, 9180-9186.
27 J. B. Goodenough and Y. Kim, Chem. Mater., 2010, **22**, 587-603.
28 M. Kim and J. H. Park, J. Power Sources, 2012, **212**, 22-27.